Turner, D. C. (1990) Ph.D. Dissertation, Princeton University, Princeton, NJ.
Turner, D. C., & Gruner, S. M. (1992) *Biochemistry* (preceding paper in this issue).
Warren, B. E. (1969) *X-ray Diffraction*, Addison-Wesley, Reading, MA.
Weiner, M. C., Suter, R. M., & Nagle, J. F. (1989) *Biophys. J. 55*, 315–325.
White, S. H., King, G. I., & Cain, J. E. (1981) *Nature 290*, 161–163.
Worcester, D. L., & Franks, N. P. (1976) *J. Mol. Biol. 100*, 359–378.

Binding of Verocytotoxin 1 to Its Receptor Is Influenced by Differences in Receptor Fatty Acid Content†

A. Pellizzari,‡,§ H. Pang,‖ and C. A. Lingwood*,‡,§,⊥,#

Department of Microbiology, The Hospital for Sick Children, 555 University Avenue, Toronto, Ontario M5G 1X8, Canada, Departments of Microbiology, Medical Genetics, and Biochemistry, University of Toronto, Toronto, Ontario M5S 1A8, Canada, and Department of Clinical Biochemistry, University of Toronto, Toronto, Ontario M5G 1L5, Canada

Received December 28, 1990; Revised Manuscript Received October 16, 1991

ABSTRACT: Globotriaosylceramide [(Galα1–4Galβ1–4Glc-ceramide (Gb_3)] was separated from human kidney, and the fatty acid composition was determined. Semisynthetic Gb_3 molecular species of corresponding fatty acid chain length were prepared and compared for verotoxin (VT) binding affinity by TLC overlay, and a quantitative binding assay was performed in the presence of auxiliary lipids. Our results indicate that, within the natural range, fatty acid chain length has little effect on verotoxin binding but that Gb_3 molecular species containing different fatty acids can interact to provide a higher affinity toxin receptor than any of the individual component receptor species. Receptor function as assayed by TLC overlay was not always found to correlate with binding in a lipid environment. Short-chain fatty acid Gb_3 molecular species could not function as VT receptors under these conditions. Evidence is presented to suggest that fatty acid chain length can have a stereoselective effect on carbohydrate conformation.

Strains of *Escherichia coli* (verotoxin-producing *E. coli*, VTEC) produce at least two immunologically distinct verocytotoxins (VT1 and VT2) that have been associated with hemorrhagic colitis (Pai et al., 1984) and the hemolytic uremic syndrome (HUS) (Karmali et al., 1985). HUS is characterized by microangiopathic hemolytic anemia and thrombocytopenia and is the leading cause of acute renal failure of children in developed countries (Karmali, 1989).

Verocytotoxins are subunit toxins made up of an active (A) subunit (MW 32 kDa) and as many as five binding (B) subunits (MW 7.7 kDa). Lingwood et al. (1987) have shown that VT1 binds specifically to glycosphingolipids such as globotriaosylceramide (Gb_3) and galabiosylceramide having a terminal Galα1–4Gal disaccharide sequence. The same glycolipid receptor has been found for VT2 (Waddell et al., 1988) and for Shiga toxin (Jacewicz et al., 1986; Lindberg et al., 1987). Gb_3 is the functional receptor for VT1 since a VT-resistant mutant Daudi cell line (Cohen et al., 1987) and a vero cell mutant (Pudymaitis et al., 1991) were found to lack Gb_3. Incorporation of Gb_3 into receptor-deficient Daudi cells resulted in the induction of VT sensitivity (Waddell et al., 1990).

Internalization of cell-bound VT1 is thought to occur by receptor-mediated endocytosis. Inside the cell the A subunit of VT1 is proteolytically nicked and reduced to the A1 fragment suppressing protein synthesis through the inhibition of elongation factor 1 dependent aminoacyl-tRNA binding to the 60S ribosome (Igarashi et al., 1987). However, the affinity of Gb_3 binding also defines cytotoxic potential of the holotoxin (Head et al., 1991).

Glycosphingolipids are components of the outer leaflet of the plasma membrane. They are thought to have roles in cell–cell interaction (Hakomori, 1981), as cell-surface receptors for some pathogenic bacteria (Stromberg et al., 1988), and function as antigens through their sugars (Marcus et al., 1981). Most attention has focused on the carbohydrate moiety of the glycolipids while the ceramide has been thought to act simply as an anchor in the plasma membrane. Studies by Kannagi et al. (1982) have shown that changes in the ceramide composition of the glycolipids were associated with variations in the reactivity of different cells with glycolipid-specific antibody. Changes in the surface exposure of sulfatide for antibody have also been shown to follow ceramide modification (Crook et al., 1986). Furthermore, the ceramide moiety of Gb_3 has been implicated in the binding of verotoxins to Gb_3 since digalactosyldiglyceride, containing the same terminal Galα1–4Gal sequence as Gb_3 and galabiosylceramide but linked to a glycerol moiety, showed no VT-binding activity (Lingwood et al., 1987; Waddell et al., 1988). Thus, the lipid portion of the molecule may affect the reactivity of glycolipids with various ligands by influencing the availability of the hydrophilic carbohydrate moiety.

Studies by Boyd and Lingwood (1989) have shown Gb_3 to be a major component of the human renal glycolipid fraction. However, changes in Gb_3 concentration could not explain the age-related incidence of HUS. If the lipid moiety were to influence binding, changes in the ceramide composition of Gb_3 might define VTEC-induced pathogenesis. The human renal

† This study was supported by Medical Research Council of Canada Grant MT 6499 and program Grant PG 11123. A.P. was the recipient of an Ontario Graduate Scholarship.

* Corresponding author.
‡ Department of Microbiology, The Hospital for Sick Children.
§ Department of Microbiology, University of Toronto.
‖ Department of Medical Genetics, University of Toronto.
⊥ Department of Clinical Biochemistry, University of Toronto.
Department of Biochemistry, University of Toronto.

0006-2960/92/0431-1363$03.00/0

Gb_3 fatty acid content was analyzed in the present study, which demonstrates that Gb_3 fatty acid microheterogeneity may play an important role in VT-induced disease.

Materials and Methods

Fatty acids, galactose oxidase, and *N,N'*-dicyclohexylcarbodiimide were from Sigma (St. Louis, MO). A monoclonal antibody reactive against Gb_3 (424/6A2) was from Biocarb (Lund, Sweden). The 96-well polystyrene microtiter plates were purchased from Nunc (Gibco BRL, Burlington, Ontario).

Extraction of Human Renal Gb_3. The ceramide trihexoside (CTH) fraction was prepared from adult human kidney by a modification of the procedure described by Strasberg et al. (1989). Human kidney obtained from an autopsy was homogenized (1 g/mL) in phosphate-buffered saline in a Waring blender. A total of 3 volumes of chloroform/methanol (C/M; 2:1 v/v) was added to the kidney suspension, and the suspension was mixed overnight at room temperature. The mixture was filtered and partitioned. The lower phase was dried, dissolved in a minimum volume of 98:2 C/M, and applied to a 25-cm (80-mL) silicic acid column (Bio-Rad) that was previously washed with 100% chloroform. Four bed volumes of chloroform were added to elute nonpolar lipids. Four volumes of acetone/methanol (A/M; 9:1) were added to elute the neutral glycosphingolipids followed by four volumes of methanol. The A/M fraction was dried. Phospholipids were removed from the mixture by saponification with 60 mL of 1 M NaOH in methanol for 2 h at 37 °C (Dawson, 1960). A Folch extraction (Folch et al., 1957) was performed, and the lower phase was collected and dried. The glycolipids were loaded on a 5-cm (15-g) silicic acid column in 98:2 C/M. The glycosphingolipids were eluted with a continuous C/M solvent gradient ranging from 10:1 C/M to 3:1 C/M such that the weights of the two starting solvents were equal. Fractions were collected, and glycolipids were resolved by TLC in a solvent system of chloroform/methanol/water (65:25:4) and visualized with orcinol. Fractions containing glycolipids with an R_f value identical to that of standard Gb_3 were collected. This CTH fraction contained three bands by TLC, and these were further separated by preparative TLC using a short-bed continuous development chamber (Regis Chemical Co., Morton Grove, IL). Continuous development TLC was performed using a solvent system of 5 mL of *n*-hexane and 25 mL of chloroform/methanol/10 mM $CaCl_2$(aq) (80:20:2). The solvent reached the lip of the tank in 5 min, and development was allowed to continue for 20 min.

Fast Atom Bombardment Mass Spectrometry (FAB-MS) and Fatty Acid Methyl Ester Analysis (FAME). All FAB spectra were obtained using the VG-Analytical ZAB-SE mass spectrometer with the 11/250 data system. The samples were dissolved in acetone or dichloromethane and were loaded onto a target containing 1–2 μL of *m*-nitrobenzyl alcohol or thioglycerol as the matrix and bombarded with xenon atoms generated using an Ion-Tech saddle field gun (8000 V, 1-mA anode current). The spectra were recorded using the multichannel analyzing (MCA) mode by exponentially scanning the magnet. The instrument was calibrated with CsI.

The samples were permethylated according to the method of Hakomori (1964) with methyl iodide and the sulfinylmethyl carbanion. The permethylated products were purified by Sephadex LH-20 chromatography in chloroform/methanol (1:1).

Fatty acid methyl ester analysis of the upper and middle bands of the Gb_3 fraction was performed by GLC as described by Myher et al. (1989).

Preparation of Deacylated Gb_3 (Lyso-Gb_3). Lyso-Gb_3 was prepared from native Gb_3 according to the method of Basta et al. (1989). Briefly, 4 mg of Gb_3 was dried under nitrogen and suspended in 10 mL of freshly prepared 1 M NaOH in methanol. The mixture was sonicated for 2 min and heated at 98 °C for 3 h. The solution was neutralized to pH 8.0 with HCl and dried. A total of 3.5 mL of 2:1 C/M was added, and the mixture was sonicated for 1 min. Salt was precipitated, and the supernatant was filtered. A Folch extraction (Folch et al., 1957) was performed to separate lyso-Gb_3 from unreacted Gb_3. The upper phase containing lyso-Gb_3 was collected, dried, and resuspended in methanol. Lyso-Gb_3 was visualized after TLC separation by ninhydrin and orcinol stains.

Semisynthetic Gb_3 Homologues. Semisynthetic Gb_3 homologues of varying fatty acid chain length were prepared using the method of Sharom and Grant (1975). Briefly, 600 μg of lyso-Gb_3 was dried under N_2 in a screw-capped test tube. A total of 6 mg of palmitic acid (C16:0) was added together with 6 mg of *N,N'*-dicyclohexylcarbodiimide. A total of 2 mL of pyridine was added, and the solution was allowed to shake overnight at room temperature under nitrogen. The same synthesis scheme was repeated for the other Gb_3 homologues (i.e., C24:1, C24:0, C22:0, C12:0, and C6:0). A total of 20 μL of the product solution was separated by TLC and sprayed with orcinol. The product was purified by silicic acid column chromatography as above using an elution gradient of 10:1 to 2:1 chloroform/methanol. Fractions containing Gb_3 were pooled.

VT1 Glycolipid Overlay. Purified glycolipids (2 μg) were separated by TLC. VT1 binding was performed as described by Lingwood et al. (1987). The plates were dried and incubated in 50 mM Tris–saline, pH 7.4 (TBS), containing 3% gelatin for 1 h, with shaking at room temperature. The plates were washed once with TBS for 5 min and incubated overnight with the verotoxin preparation (0.12 μg/mL). The plates were washed three times with TBS and incubated with 0.025% polyclonal rabbit anti-VT1 for 2 h at room temperature. The plates were washed three times with TBS and further treated with peroxidase-conjugated goat anti-rabbit IgG for 2 h at room temperature. The plates were washed three times with TBS, and glycolipid-bound toxin was visualized with 4-chloro-1-naphthol peroxidase substrate. The reaction was terminated by extensive washing with distilled water.

Microtiter Plate VT1–Gb_3 Binding Assay. A modification of the procedure of Kannagi et al. (1982) was used. Glycolipid (100 μL containing 100 ng of Gb_3) in a methanolic solution containing phosphatidylcholine and cholesterol in a ratio of 1:5:2.5 by weight was added to microtiter plates and allowed to evaporate overnight. The plate was blocked with 100 mM TBS (pH 7.4) containing 3% BSA for 2 h at room temperature and washed once with TBS containing 0.1% BSA. A total of 50 ng of ^{125}I-VT1, labeled by iodogen catalysis (10 000 cpm/well) (kindly provided by S. Head, Department of Microbiology, The Hospital for Sick Children), plus increasing concentrations of unlabeled VT were added to the wells in triplicate for 2 h at 25 °C. The wells were washed 10 times with 100 mM TBS, pH 7.4, containing 0.1% BSA, cut out, and counted in a γ-counter (Beckman).

Galactose Oxidase Labeling of Gb_3 in Microtiter Plates. Labeling of the terminal galactose residue of Gb_3 immobilized in microtiter plates was performed as follows: 500 ng of a Gb_3 homologue in a methanol solution of phosphatidylcholine and cholesterol as above was dried in microtiter wells. Labeling was performed using the method of Okada et al. (1985).

Briefly, 0.5 unit of galactose oxidase (Sigma) in PBS, pH 7.0, was added to each well (50 μL/well) and allowed to incubate for 1 h at 37 °C. The wells were washed three times with PBS. A total of 25 μCi of tritiated $NaBH_4$ (ICN Radiochemicals) was added, and the wells were allowed to stand at room temperature for 1 h. The wells were washed three times with cold $NaBH_4$ and washed five times with PBS. A total of 200 μL of methanol was added to each well, and the wells were sonicated in a water bath for 10 min. The solution was added to a scintillation vial together with a subsequent 200-μL methanol wash. Scintillant was added, and the vials were counted. Control wells containing only PC and cholesterol and Gb_3-containing wells in which galactose oxidase was omitted were included.

Anti-Gb_3 TLC Overlay. CTH samples were applied to TLC sheets and separated in 65:25:4 C/M/W (v/v/v). The plates were dried and blocked with 3% gelatin in 100 mM TBS (pH 7.4) for 1 h at 37 °C. The plate was washed once and incubated with a monoclonal IgM directed against the Galα1–4Galβ1–4Glc carbohydrate epitope for 2 h at room temperature. The plate was washed three times and then incubated with goat anti-rabbit HRP conjugate and developed as above.

α-Galactosidase Digestion of Globotriaosylceramide. A total of 20 μg of Gb_3 was dried in a screw-capped tube and dissolved in 0.2 mL of 50 mM sodium citrate buffer (pH 4.5) containing 2 mM EDTA, 1% BSA, and 500 μg of taurodeoxycholic acid. The preparation was sonicated for 30 s, and 0.5 unit of coffee bean α-galactosidase (Sigma) was added, and the mixture was incubated at 37 °C overnight. The incubation mixture was partitioned (Folch et al., 1957), and the lower phase was dried and resolved on TLC.

Results

Characterization of Human Renal Gb_3 Species. The Gb_3 species of human renal tissue were purified by silicic acid chromatography essentially by the method of Strasberg et al. (1989) using a gradient of 10:1 CM to 3:1 CM. The ceramide trihexoside fraction was further separated using a continuous TLC development chamber resulting in the resolution of three CTH species (Figure 1). These species were subject to α-galactosidase digestion. Figure 1 shows the formation of lactosylceramide from the upper and middle band of the CTH fraction. However, the lower band in the CTH fraction was not susceptible to α-galactosidase digestion. Moreover, VT1 and monoclonal IgM directed against the Galα1–4Gal carbohydrate epitope recognized the upper and middle band of the CTH fraction but not the lower species (Figure 1). Thus, the lower band was determined not to be Gb_3 or Gb_4 according to conventional TLC in 65:25:4 chloroform/methanol/water (v/v) (data not shown).

Fast Atom Bombardment Mass Spectrometry (FAB-MS). The FAB mass spectrum of the underivatized upper band isolated from the CTH fraction demonstrated sodiated molecular ions at m/z 1156 and m/z 1154, which correspond to Hex_3-ceramide. The presence of fragment ions m/z 282, 280 and 264, 262 indicated the presence of both sphingosine and dihydrosphingosine. The fatty acid C24:1 was the major fatty acid component of the glycosphingolipid as evidenced by the fragment ions m/z 630, 628 and the molecular ions m/z 1156, 1154. The FAB mass spectrum of the permethylated sample is shown in Figure 2. The sodiated molecular ions at m/z 1324, 1322 represented an addition of 12 methyl groups upon permethylation and agreed with the composition of Hex_3-ceramide. The fragment ions m/z 1270 (MH MeOH), m/z 1066 (m/z 1270, hexose), m/z 862 (m/z 1066, hexose), and m/z 658 (m/z 862, hexose) confirmed the presence of three

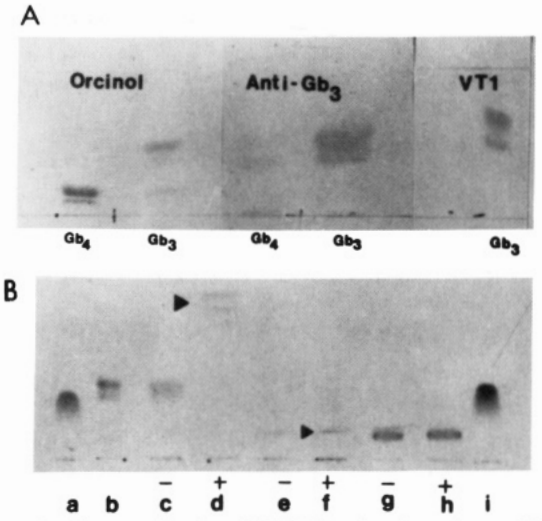

FIGURE 1: Characterization of CTH fraction from human kidney. The CTH fraction, separated by silicic acid chromatography, was resolved by TLC in a continuous development chamber (see Materials and Methods). (A) Immunostaining: The ceramide trihexoside (Gb_3) and ceramide tetrahexoside (Gb_4) fraction were stained with anti-Gb_3 or VT1 + anti-VT1 as indicated. (B) α-Galactosidase digestion: The lanes represent (a and i) sulfogalactosyl-glycerolipid standard; (b, c, and d) renal CTH fraction, (e and f) isolated lower band from CTH fraction, and (g and h) ceramide tetrahexoside fraction. Plus and minus refer to incubations performed with and without α-galactosidase, respectively. Arrows indicate digestion product of upper and middle band Gb_3 (lane d) and resistance of the lower band (lane f) to α-galactosidase.

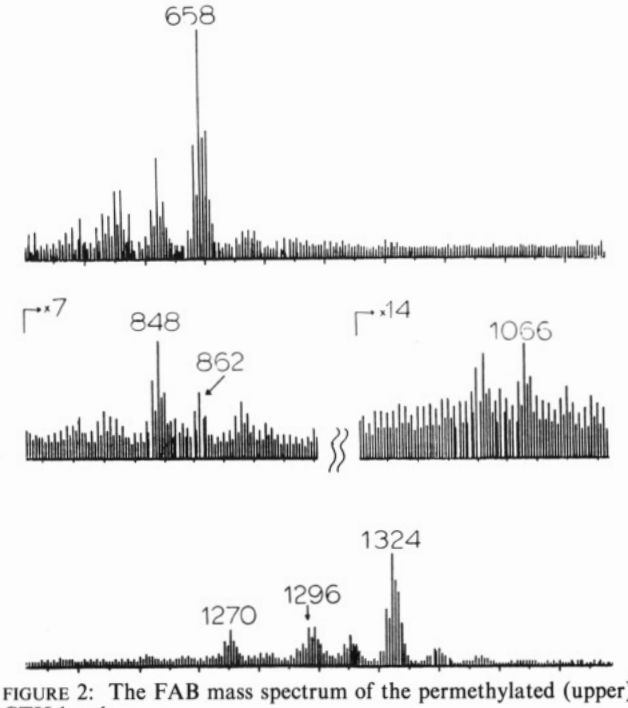

FIGURE 2: The FAB mass spectrum of the permethylated (upper) CTH band.

hexoses and a ceramide group. A summary of the observed fragment ions is shown:

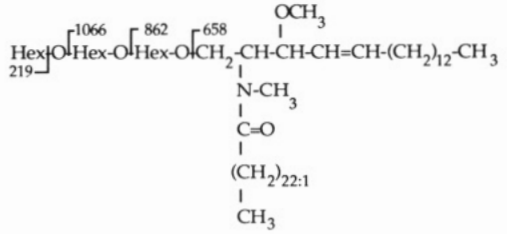

Table I: Fatty Acid Methyl Ester Analysis (FAME) of Renal Gb_3[a]

FAME (nonhydroxy)	middle band area %	upper band area %
14:0	4.62	2.45
16:0	42.11	10.47
16:1	3.12	1.58
17:0	1.21	0.46
18:0	18.98	5.20
18:1Ω9	6.17	3.24
18:2Ω6	1.72	1.05
20:0	6.42	3.91
20:1Ω9	0.00	0.00
21:0	0.22	0.18
22:0	6.46	16.41
20:4Ω6	0.47	1.30
22:1Ω9	0.60	1.18
23:0	0.52	1.64
24:0	2.67	17.29
24:1	3.86	32.10
other	0.85	1.55

[a] Upper and middle refer to the migration of the Gb_3 doublet by conventional TLC isolated from the CTH fraction. The middle Gb_3 band contained predominantly C16:0 and C18:0 fatty acids while the upper band contained mostly C24:1, C24:0, and C22:0 fatty acids. All fatty acids were nonhydroxylated. Fatty acid analysis was performed as described by Myher et al. (1989).

The FAB mass spectrum of the underivatized middle band gave a sodiated molecular ion at m/z 1046 which represented a Hex_3-ceramide with sphingosine as the base and C16:0 fatty acid as the major component. Permethylation produced a sodiated molecular ion at m/z 1214 (an addition of 12 methyl groups).

GLC Fatty Acid Analysis. The fatty acid analyses of the purified renal upper and middle band Gb_3 are shown in Table I. The major fatty acids in the upper band were predominantly C24:1, C24:0, and C22:0 and those in the lower band were C16:0 and C18:0. No hydroxy fatty acids were detected, indicating that the longer chain length must explain the difference in TLC migration.

VT1 Binding to Gb_3 Homologues. The fatty acid had a significant effect on the ability of the carbohydrate moiety of Gb_3 to act as a receptor for VT1 in the lipid matrix of the microtiter plates (Figure 3). VT1 did not readily bind lyso-Gb_3 under these conditions despite the fact that effective binding on TLC plates was observed (See Figure 5). A 25–50-fold increase in lyso-Gb_3 was needed to bind equivalent amounts of toxin as upper and middle band Gb_3.

In order to determine the effect that Gb_3 fatty acid chain length had on VT1 binding, it was necessary to obtain Gb_3 species with homogeneous fatty acid content. A series of Gb_3 homologues were synthesized from lyso-Gb_3 to determine their affinity for VT1. These homologues, containing C6:0, C12:0, C16:0, C22:0, C24:0, and C24:1, were separated by TLC and initially compared with the separated human renal Gb_3 bands (Figure 4). All species were efficiently bound by VT1 in the TLC overlay assay (Figure 5).

The effect of the fatty acid on the kinetics of VT1 binding was determined using the quantitative microtiter assay. Using this assay, addition of ^{125}I-VT1 resulted in a saturable binding curve (Figure 3). Bound ^{125}I-VT1 was measured and analysis of the data was performed by the LIGAND computer program developed by Munson and Rodbard (1980). This program provided estimates of affinity constants and binding capacities through a least-squares curve-fitting program, thus avoiding potential biases introduced by graphical approximations from Scatchard plots. The results are presented in Table II. Some variation in the binding affinity of the natural Gb_3 species was observed between different preparations, but the middle band

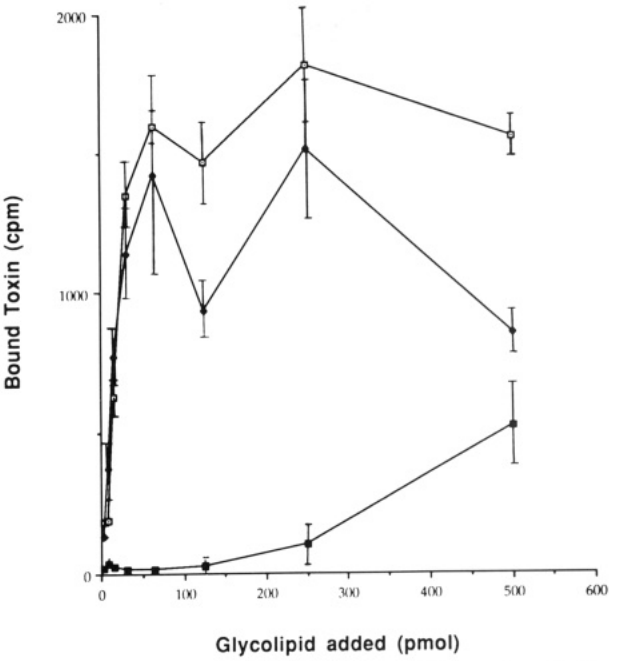

FIGURE 3: Quantitation of VT1 binding to renal Gb_3 species. Binding of 50 ng of ^{125}I-VT1 to glycolipids adsorbed together with auxiliary lipids in microtiter wells was determined as described under Materials and Methods: □, upper band renal Gb_3; ◆, middle band Gb_3; ■, lyso-Gb_3.

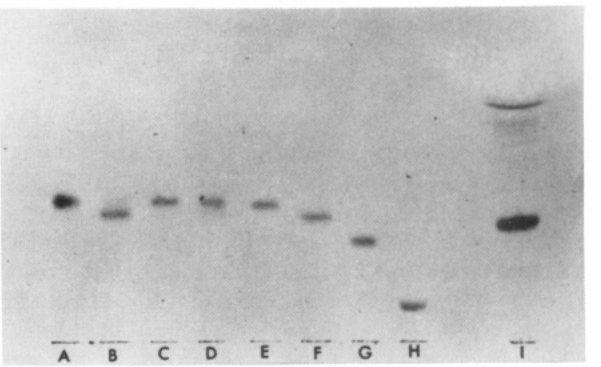

FIGURE 4: TLC of natural and semisynthetic Gb_3 homologues visualized with orcinol. Lanes: (A) Gb_3 (upper band from human kidney); (B) Gb_3 (middle band from human kidney); (C–I) the semisynthetic Gb_3 homologues (C) C24:1, (D) C24:0, (E) C22:0, (F) C16:0, (G) C6:0, (H) lyso-Gb_3 (deacylated Gb_3), and (I) C12:0. A total of 2 μg of the homologues was dotted in each lane. Lane I shows the crude reaction mixture before the C12:0 homologue was purified from excess reactants. Note that all of the initial lyso-Gb_3 has been converted to product (see Materials and Methods).

showed consistent higher affinity. There was little difference in the affinity of VT1 binding to the homogeneous semisynthetic Gb_3's (C12 → C24). The association constants were ~20 μM^{-1} (that of C22 Gb_3 was a little lower). (Lyso-Gb_3 and C6:0-containing Gb_3 did not bind VT1 in the microtiter assay under these conditions). Affinity constants for middle band of renal Gb_3 were, however, significantly higher. The middle band Gb_3 (comprising mainly the C16 species) showed increased affinity for the toxin as compared with the C16:0 homologue, while the K_a of the upper band was within the range of the longer chain semisynthetic homologues of which it was composed. A one-ligand–one-site model best described the above data, for both the semisynthetic and renal Gb_3 species (Table II).

However, when an equimolar mixture of four of the semisynthetic Gb_3 homologues was assayed, a two-site binding

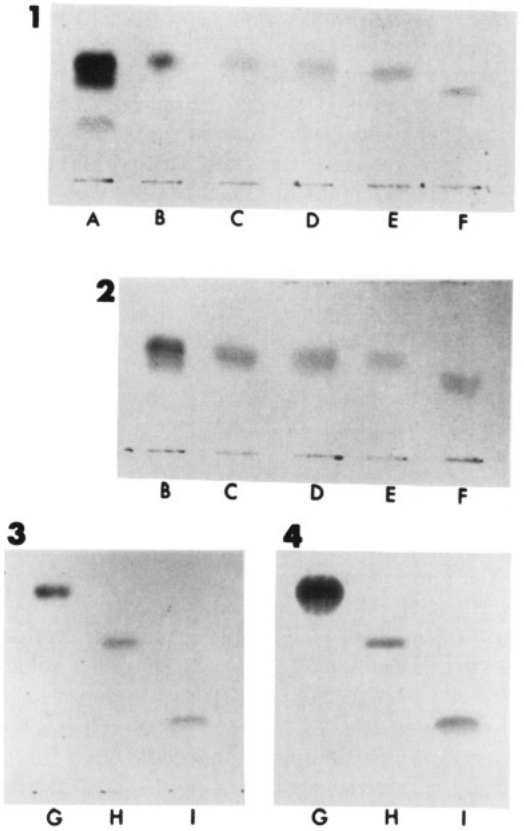

FIGURE 5: VT1 TLC overlay binding to Gb_3 homologues. Plates 1 and 3 are visualized by orcinol spray while plates 2 and 4 are visualized by VT1 binding. Lanes: (A) total CTH fraction from human kidney, (B) renal Gb_3 (upper band), (C) C24:1 Gb_3, (D) C22:0 Gb_3, (E) C24:0 Gb_3, (F) C16:0 Gb_3, (G) renal Gb_3 (upper band), (H) C6:0 Gb_3, (I) lyso-Gb_3. A total of 1 μg was applied in lanes B–I.

Table II: VT1 Binding to Gb_3 Homologues: Estimates of Binding Parameters as Determined by LIGAND[a]

	K_a (μM^{-1})	R_1 (nM)
1 renal Gb_3[b] (upper)	7.8 ± 2.6	46.1 ± 11.6
	21.7 ± 4.0	31.2 ± 3.5
2 renal Gb_3[b] (middle)	55.4 ± 31.6	0.95 ± 0.2
	115 ± 107	2.42 ± 0.6
3 C12:0 Gb_3[b]	24.3 ± 7.7	3.0 ± 1.7
4 C16:0 Gb_3[b]	26.3 ± 9.7	3.15 ± 0.6
	28.0 ± 17.0	5.5 ± 1.9
	av 27.2 ± 17.2	av 4.3 ± 2.3
5 C22:0 Gb_3[b]	10.3 ± 4.9	9.6 ± 3.3
	15.0 ± 3.9	12.9 ± 2.3
	av 12.7 ± 6.8	av 11.3 ± 4.3
6 C24:0 Gb_3[b]	26.0 ± 7.5	2.4 ± 0.4
	31.3 ± 10.9	5.41 ± 1.04
	av 28.7 ± 12.9	av 3.9 ± 0.9
7 C24:1 Gb_3[b]	21.3 ± 9.7	4.6 ± 1.2
	20.2 ± 3.4	12.2 ± 1.3
	av 20.8 ± 10.1	av 8.4 ± 2.3
8 Gb_3 mixture[c] (C16,22,24,24:1)	89.8 ± 71.9 (first site)	1.8 ± 1.1 (first site)
	1.7 ± 6.7 (second site)	7.9 ± 21.0 (second site)

[a] Two experiments were performed for entries 1, 2, and 4–7. Different preparations of upper and middle renal Gb_3 were used, and the average was therefore not determined. [b] Best fits a one-ligand–one-site model. [c] Best fits a one-ligand–two-site model.

model with a second affinity higher than any of the individual binding affinities was found to best fit the data (Table II). The affinity of this second binding site was within the range observed for the middle renal Gb_3 species. Further, varying the proportions in a C16:0 and C24:0 fatty acid containing Gb_3

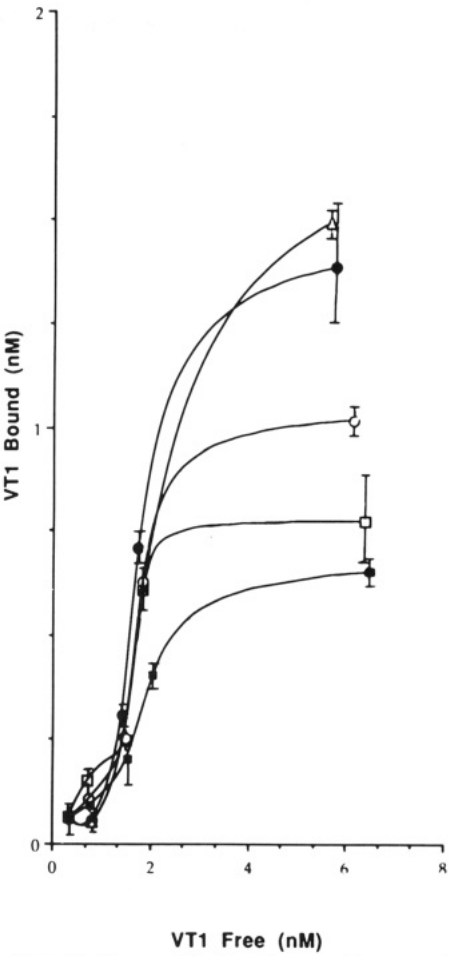

FIGURE 6: VT1 binding to Gb_3 homologue mixtures. Increasing concentrations of semisynthetic C16:0 and C24:0 Gb_3's were mixed together in the following ratios: 100% C16:0 (■), 100% C24:0 (□), 75% C16:0 and 25% C24:0 (○), 50% C16:0 and 50% C24:0 (△), 25% C16:0 and 75% C24:0 (●). The mixtures were immobilized in microtiter plates together with auxiliary lipids and tested for ^{125}I-VT1 binding.

mixture resulted in a marked increase in the amount of toxin bound relative to either species alone (Figure 6). The ratio within the mixture defined the affinity (slope) and number of binding sites (plateau) of the binding curve.

Comparison of Galactose Oxidase Labeling and VT1 Binding. The extent of terminal α-galactose exposure of the Gb_3 homologues in the lipid environment of the microtiter well was determined by galactose oxidase labeling (Figure 7). Such labeling was compared to VT1 binding in a duplicate series of wells. Lyso-Gb_3 and Gb_3 containing the C6:0 fatty acid were not susceptible to galactose oxidase or to VT1 binding. The free amino group of lyso-Gb_3 did not inhibit binding per se since strong binding to lyso-Gb_3 was observed in the absence of auxiliary lipids (Relisa format; Basta et al., 1989). The next three homologues (C12:0,C16:0, C22:0) were increasingly susceptible to galactose oxidase and VT1. However, the C24:0 and C24:1 Gb_3 homologues were not susceptible to oxidation but they remained effective ligands for VT1 (Figure 7).

DISCUSSION

Although infection with verotoxin-producing *E. coli* is a primary determinant in the etiology of the hemolytic uremic syndrome (Karmali, 1989), the factors which determine the pathology (diarrhea, bloody diarrhea, or the more severe sequellae of HUS) following such an infection are unknown.

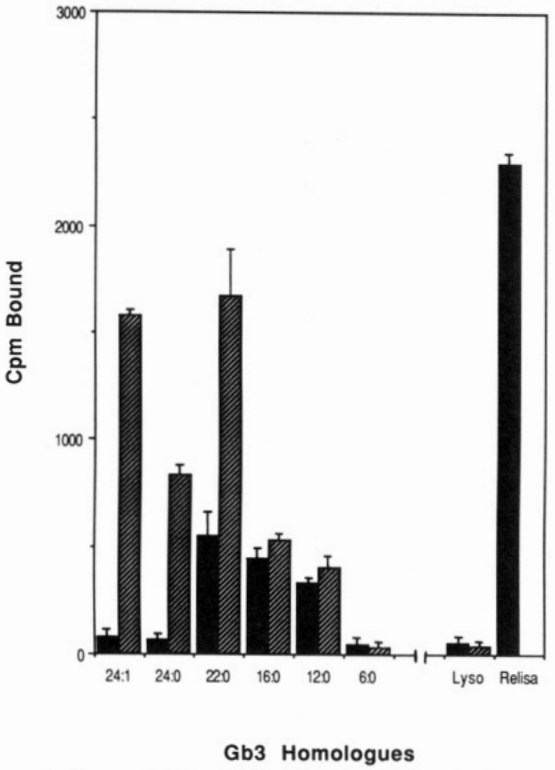

FIGURE 7: Susceptibility of Gb_3 homologues to galactose oxidase labeling and binding to VT1. Galactose oxidase radiolabeling and ^{125}I-VT1 binding was compared for Gb_3 homologues adsorbed with auxiliary lipids in microtiter wells as described under Materials and Methods. Relisa involved the sensitization of microtiter wells with lyso-Gb_3 alone using the method of Basta et al. (1989). Solid bars: galactose oxidase/NaB^3H_4 labeling. Hatched bars: ^{125}I-VT1 binding.

Since the functional receptor for the toxin has been identified as the glycolipid Gb_3 (Cohen et al., 1987; Waddell et al., 1990; Sandvig et al., 1991), our laboratory has been interested in determining whether any differential expression of this glycolipid, for example, containing a specific fatty acid, might preferentially bind VT and thus predispose any individual to HUS following VTEC infection. We have already shown the importance of the lipid moiety in that Galα1–4Gal glycerolipid, unlike the corresponding glycosphingolipid, is not bound by VT (Lingwood et al., 1987; Waddell et al., 1988).

Gb_3 is the P^k antigen of the P blood group, and it has been shown that individuals lacking the P1 glycolipid antigen (also containing a terminal Galα1–4Gal residue and binding VT) show a higher incidence of HUS following VTEC infection (Taylor et al., 1989). It was postulated that the P1 antigen on circulating red blood cells might serve to "mop up" any systemic toxin and thus prevent renal damage following gastrointestinal infection. We have found, however, that verotoxin does not bind to human red blood cells irrespective of their P blood group status. Thus, despite the presence of Gb3 and P1 in these cells and their use as cell-surface-typing antigens, they are unavailable for VT binding.

In our initial approach to determine what factors can influence the ability of Gb_3 to act as a membrane receptor for verotoxin, we decided to study the fatty acid composition of human renal Gb_3 and its effect on VT binding.

The species in the human renal ceramide trihexoside fraction were separated and characterized by reaction with anti-Gb_3 antibodies, α-galactosidase digestion, and reactivity with VT1 (Figure 1). Two species which bound VT and were susceptible to α-galactosidase were separated. A third CTH species with a lower R_f was detected by orcinol only. Globotriaosylceramide was confirmed by mass spectroscopy for the upper two species only. The fatty acids of the upper and middle CTH bands were determined by GLC analysis of the methyl esters (Table I), and the major species was confirmed by FAB mass spectroscopy. The lower band was not Gb_3 and was not characterized further. The upper band was Gb_3 containing fatty acid chain lengths of C22:0, C24:0, and C24:1. The middle band contained primarily C16:0 fatty acid. These analyses correlated with the expected migration of Gb_3 on TLC. No hydroxylated fatty acids were detected by GLC. This could not be confirmed by mass spectroscopy since a 16-mass-unit increase could also arise from a potassium as opposed to sodium adduct ion fragment. These data are nevertheless essentially the same as previous studies on the fatty acid composition of human renal Gb_3 (Martensson, 1966).

The affinity of the upper and middle band Gb_3 for VT1 binding was significantly different by LIGAND analysis (Table II). The middle band showed high affinity but low capacity while the upper band showed somewhat lower affinity but higher capacity. Our recent studies have shown that the affinity of VT binding to Gb_3 can determine the cytotoxicity of VT in vitro (Head et al., 1991) and may thus relate to the cytopathology observed in vivo.

The semisynthetic Gb_3's corresponding to the major fatty acid species present in upper and middle band Gb_3 were all effectively recognized by VT1 using the TLC overlay assay (Figure 5). Analysis by LIGAND (Table II) of the binding of ^{125}I-VT1 to the semisynthetic Gb_3's indicated that the binding affinity (K_a) was not significantly different for any of the homologues, even C12. Slightly lower binding affinity was observed for C22 Gb_3, and this as yet remains unexplained. Thus, altering fatty acid composition per se (chain length and degree of saturation) had little effect on recognition of VT1. A one-ligand–one-site model provided the best fit for VT1 binding to the individual Gb_3 species and the upper and lower renal species. In the case of the upper band, the affinity was similar to those of its composite Gb_3 molecular species. However, middle Gb_3 (containing 42% C16) showed higher K_a values than the corresponding C16:0 homologue. This was interpreted to suggest that the heterogeneous component within this species may be responsible for the increased affinity by a cooperative binding effect.

In a preliminary approach to test such a possibility, we prepared an equimolar mixture of four semisynthetic compounds and determined the effect on VT binding affinity. This resulted in the generation of an additional binding site of higher affinity than any of the individual species alone (Table II). This suggests that indeed the different fatty acid containing Gb_3 species can interact cooperatively to increase VT binding affinity. Although the affinity was markedly increased for the mixture, we were unable to mimic the capacity of binding observed for the upper Gb_3 species. This is interpreted to suggest that the exact ratio of components within the Gb_3 mixture is important. This hypothesis was supported by subsequent experiments to determine the binding of VT1 to C16:0 and C24:0 Gb_3 mixed together in various ratios (Figure 6). The binding curve for the mixtures showed a higher binding saturation and increased slope than either of the homogeneous receptors. Thus, both the affinity and number of receptor sites available (capacity) can increase for isoreceptor mixtures. The ratio within the mixture is important since a mixture of 25% C16/75% C24 was most effective in this experiment. We would expect more complex cooperative kinetics would be observed for more intricate Gb_3 mixtures,

and this in turn might be more pronounced in a plasma membrane environment.

The cooperative Gb_3 binding we have observed may also explain the findings of Jacewicz et al. (1989), who speculated that Gb_3 species in HeLa cells might interact in a cooperative fashion to provide a second toxin-binding site of higher affinity.

The increased affinity due to cooperative binding of isoreceptors present in Gb_3 of mixed fatty acid content may result from the ability of such mixtures to present a nonplanar "receptor surface" to better fit the three-dimensional configuration of the pentameric binding site of the holotoxin. The change in capacity is more difficult to explain but might result from an increased lateral mobility to more efficiently accommodate the pentavalent toxin.

In a lipid environment, the fatty acid of Gb_3 is crucial for binding. Approximately 25–50 times more lyso-Gb_3 was needed, compared with the amount of the longer chain fatty acid containing Gb_3, to bind equivalent amounts of toxin (Figure 3). The influence of fatty acid content on the ability of receptor to bind VT was dramatically illustrated in the C6:0-containing Gb_3 species. Using the TLC overlay binding procedure, the C6:0 Gb_3, together with lyso-Gb_3, was effectively recognized by VT (Figure 5). However, when included with auxiliary lipids in the microtiter binding assay, no binding of VT1 to these species was observed (Figure 7). Thus, there is a cutoff in fatty acid chain length to allow binding to Gb_3 in a lipid mixture. TLC binding data cannot therefore always be directly correlated with the ability of a given species to serve as a cell membrane receptor. Direct immobilization of lyso-Gb_3 in microtiter wells in the absence of other lipids, as we have used for the development of a highly sensitive Relisa system for the rapid detection of VT (Basta et al., 1989), results in the efficient recognition of VT1, indicating that the free amine has no adverse effect on VT binding. Indeed, under these conditions lyso-Gb_3 is the best receptor and is able to bind lower concentrations of VT (Basta et al., 1989) than Gb_3 itself (Ashenazi & Cleary, 1989).

Our results illustrate another important effect. Comparison of the ability of Gb_3's of increasing fatty acid chain length to serve as a substrate for galactose oxidase (commonly used to access the "exposure" of the glycolipid) and to bind VT shows good correlation for the short- and middle-length fatty acids. However, the longer fatty acid chain Gb_3's remain effective toxin receptors but are not labeled by galactose oxidase. "Exposure" is therefore a relative term and must be interpreted only in relation to the binding ligand used. The C3 position of the terminal α-galactose residue is important for VT binding (Lingwood et al., 1987), whereas galactose oxidase modifies the C6 position which must be "masked" in the long-chain fatty acid Gb_3 species. Thus, changes in glycolipid fatty acid composition can change, not only the availability or exposure of the carbohydrate receptor, but also the overall orientation of the terminal carbohydrate moiety, which may profoundly affect its receptor function.

Our data therefore indicate that the fatty acid content of human renal Gb_3 may play a role in determining the binding affinity of VT to renal target cells and may thus influence the possible clinical consequences of VTEC infection.

Acknowledgments

We thank Dr. A. Kuksis, Banting and Best Department of Medical Research, University of Toronto, for GLC analysis of the fatty acid content of renal Gb_3. Mass spectral analyses were performed at the Toronto Carbohydrate Centre.

Registry No. C14:0, 544-63-8; C16:0, 57-10-3; C16:1, 373-49-9; C17:0, 506-12-7; C18:0, 57-11-4; C18:1Ω9, 112-80-1; C18:2Ω6, 60-33-3; C20:0, 506-30-9; C20:1Ω9, 5561-99-9; C21:0, 2363-71-5; C22:0, 112-85-6; C20:4Ω6, 506-32-1; C22:1Ω9, 112-86-7; C23:0, 2433-96-7; C24:0, 557-59-5; C24:1, 31152-46-2.

References

Ashenazi, S., & Cleary, T. G. (1989) *J. Clin. Microbiol. 27*, 1145–1150.

Basta, M., Karmali, M., & Lingwood, C. A. (1989) *J. Clin. Microbiol. 27*, 1617–1622.

Boyd, B., & Lingwood, C. A. (1989) *Nephron 51*, 207–210.

Calderwood, S. B., Auclair, F., Donohue-Rolfe, A., Keusch, G. T., & Mekalanos, J. J. (1987) *Proc. Natl. Acad. Sci. U.S.A. 84*, 4364–4368.

Cohen, A., Hannigan, B., Williams, R. G., & Lingwood, C. A. (1987) *J. Biol. Chem. 262*, 17088–17091.

Crook, S. J., Boggs, J. M., Vistnes, A. I., & Koshy, K. M. (1986) *Biochemistry 25*, 7488–7494.

Dawson, R. M. C. (1960) *Biochem. J. 75*, 45–49.

Folch, J., Lees, M., & Sloane-Stanley, G. H. (1957) *J. Biol. Chem. 226*, 497–509.

Hakomori, S.-I. (1964) *J. Biochem. 55*, 205–208.

Hakomori, S.-I. (1981) *Annu. Rev. Biochem. 50*, 733–764.

Head, S., Karmali, M., & Lingwood, C. A. (1991) *J. Biol. Chem. 266*, 3617–3621.

Igarashi, K., Ogasawara, T., Ito, K., Yutsudo, T., & Takeda, Y. (1987) *FEMS Microbiol. Lett. 44*, 91–94.

Jacewicz, M., Clausen, H., Nudelman, E., Donohue-Rolfe, A., & Keusch, G. T. (1986) *J. Exp. Med. 163*, 1391–1404.

Jacewicz, M., Feldman, H. A., Donohue-Rolfe, A., Balasubramanian, K. A., & Keusch, G. T. (1989) *J. Infect. Dis. 159*, 881–889.

Kannagi, R., Nudelman, E., & Hakomori, S. (1982) *Proc. Natl. Acad. Sci. U.S.A. 79*, 3470–3474.

Karmali, M. A. (1989) *Clin. Microbiol. Rev. 2* (1), 15–38.

Karmali, M. A., Petric, M., Lim, C., Fleming, P. C., Arbus, G. S., & Lior, H. (1985) *J. Infect. Dis. 151*, 775–782.

Lindberg, A. A., Brown, J. E., Stromberg, N., Westling-Ryd, M., Schultz, J. E., & Karlsson, K. A. (1987) *J. Biol. Chem. 262*, 1779–1785.

Lingwood, C. A. (1979) *Can. J. Biochem. 57*, 1138–1143.

Lingwood, C. A., Law, H., Richardson, S., Petric, M., Brunton, J. L., DeGrandis, S., & Karmali, M. (1987) *J. Biol. Chem. 262*, 8834–8839.

Marcus, D. M., Kundu, S. K., & Suzuki, A. (1981) *Hematology 18*, 63–71.

Martensson, E. (1966) *Biochim. Biophys. Acta 116*, 296–308.

Mobassaleh, M. A., Donohue-Rolfe, A., Jacewicz, M., Grand, R. J., Keusch, G. T. (1988) *J. Infect. Dis. 157*, 1023–1031.

Morrison, D. M., Tyrell, D. L. J., & Jewell, L. D. (1985) *Am. J. Clin. Pathol. 86*, 108–112.

Munson, P. J., & Rodbard, D. (1980) *Anal. Biochem. 107*, 220–239.

Myher, J. J., Kuksis, A., & Pind, S. (1989) *Lipids 24*, 396–407.

O'Brien, A. D., LaVeck, G. D., Thompson, M. R., & Formal, S. B. (1982) *J. Infect. Dis. 144*, 694–696.

Okada, Y., Arima, T., & Nagashima, H. (1985) *Anal. Biochem. 147*, 311–314.

Pai, C. H., Gordon, R., Sims, H. V., & Bryan, L. E. (1984) *Ann. Intern. Med. 101*, 738–742.

Pudymaitis, A., Armstrong, G., & Lingwood, C. A. (1991) *Arch. Biochem. Biophys. 286*, 448–452.

Sandvig, K., Olsnes, S., Brown, J. E., Petersen, O. W., & van Deurs, B. (1989) *J. Cell Biol. 108*, 1331–1343.

Sandvig, K., Prydz, K., Ryd, M., & van Deurs, B. (1991) *J. Cell Biol. 113*, 553–562.

Sharom, F. J., & Grant, C. W. M. (1975) *Biochem. Biophys. Res. Commun. 67*, 1501–1506.
Strasberg, P., Grey, A., Warren, I., & Skomorowski, M.-A. (1989) *J. Lipid Res. 30*, 121–127.
Stromberg, N., Ryd, M., Linberg, A. A., & Karlsson, K. A. (1988) *FEBS Lett. 232*, 193–198.
Taylor, C. M., Milford, D. V., Rose, P. E., Roy, T. C., & Rowe, B. (1990) *Pediatr. Nephrol. 4*, 59–61.
Waddell, T., Head, S., Petric, M., Cohen, A., & Lingwood, C. (1988) *Biochem. Biophys. Res. Commun. 152*, 674–679.
Waddell, T., Cohen, A., & Lingwood, C. A. (1990) *Proc. Natl. Acad. Sci. U.S.A. 87*, 7898–7901.

Substitution of *Torpedo* Acetylcholine Receptor α1-Subunit Residues with Snake α1- and Rat Nerve α3-Subunit Residues in Recombinant Fusion Proteins: Effect on α-Bungarotoxin Binding†

Vijaya Chaturvedi, Diana L. Donnelly-Roberts, and Thomas L. Lentz*
Department of Cell Biology, Yale University School of Medicine, New Haven, Connecticut 06510
Received August 16, 1991; Revised Manuscript Received November 12, 1991

ABSTRACT: A fusion protein consisting of the TrpE protein and residues 166–211 of the *Torpedo* acetylcholine receptor α1 subunit was produced in *Escherichia coli* using a pATH10 expression vector. Residues in the *Torpedo* sequence were changed by means of oligonucleotide-directed mutagenesis to residues present in snake α1 subunit and rat nerve α3 subunit which do not bind α-bungarotoxin. The fusion protein of the *Torpedo* sequence bound ^{125}I-α-bungarotoxin with high affinity (IC_{50} = 2.5 × 10^{-8} M from competition with unlabeled toxin, K_D = 2.3 × 10^{-8} M from equilibrium saturation binding data). Mutation of three *Torpedo* residues to snake residues, W184F, K185W, and W187S, had no effect on binding. Conversion of two additional *Torpedo* residues to snake, T191S and P194L, reduced α-bungarotoxin binding to undetectable levels. The P194L mutation alone abolished toxin binding. Mutation of three *Torpedo* α1 residues to neuronal α3-subunit residues, W187E, Y189K, and T191N, also abolished detectable α-bungarotoxin binding. Conversion of Tyr-189 to Asn which is present in the snake sequence (Y189N) abolished toxin binding. It is concluded that in the sequence of the α subunit of *Torpedo* encompassing Cys-192 and Cys-193, Tyr-189 and Pro-194 are important determinants of α-bungarotoxin binding. Tyr-189 may interact directly with cationic groups or participate in aromatic–aromatic interactions while Pro-194 may be necessary to maintain a conformation conducive to neurotoxin binding.

The nicotinic acetylcholine receptor (AChR)[1] of skeletal muscle and fish electric organ is a pentamer composed of two α1 subunits and β, γ, and δ subunits [reviewed in Karlin et al. (1986), McCarthy et al. (1986), Stroud et al. (1990), and Galzi et al. (1991)]. Binding of the neurotransmitter acetylcholine (ACh) induces transient opening of a channel, allowing sodium ions to enter the cell. Identification of the agonist-binding site on the receptor has been facilitated by the use of snake venom curaremimetic neurotoxins, such as α-bungarotoxin (α-Btx), which bind specifically and with high affinity to the AChR and competitively block the binding of ACh [see Lentz and Wilson (1988)]. Studies of the binding of α-Btx to synthetic peptides of the α1 subunit have demonstrated toxin binding to residues 173–204 (Wilson et al., 1985, 1988; Wilson & Lentz, 1988), 182–198 (Mulac-Jericevic & Atassi, 1986), 185–196 (Neumann et al., 1986a,b), 172–205 and 185–199 (Ralston et al., 1987), 188–201 (Gotti et al., 1988), 183–200 (Takamori et al., 1988), 181–200 (Conti-Tronconi et al., 1990), 185–196 and 181–198 (Pearce & Hawrot, 1990), 185–199 (Griesmann et al., 1990), and 172–227 (Donnelly-Roberts & Lentz, 1991). These studies indicate a major neurotoxin determinant is located in a region of the primary sequence flanking Cys-192 and Cys-193. These cysteines are labeled by affinity alkylating agents and are considered to lie close to the ACh-binding site (Kao et al., 1984; Dennis et al., 1986). In addition to synthetic peptides, recombinant toxin-binding proteins have been utilized to investigate the toxin-binding site. Fusion proteins containing α1-subunit residues 160–216 (Barkas et al., 1987), 166–200 (Gershoni, 1987), 184–200 and 184–196 (Aronheim et al., 1988), and 183–204 (Ohana & Gershoni, 1990) bind α-Btx, confirming the findings with synthetic peptides.

As a first step in understanding how binding of agonists leads to opening of the ion channel, it is necessary to gain knowledge of structure–function relationships of the binding site. Some information can be obtained by comparison of sequences from species which bind neurotoxins with different affinities. For example, in a study of α-Btx binding to a synthetic peptide comprising residues 173–204 of the α1 subunit, the affinity for the corresponding calf peptide was 15-fold less than for the *Torpedo* peptide, and for the human peptide, 150-fold less (Wilson & Lentz, 1988). The rank order of decreasing affinity (K_D) for α-Btx binding to fusion proteins containing residues 183–204 is *Torpedo*, chick, *Xenopus*, *Drosophila*, mouse, calf, and human (Ohana & Gershoni, 1990). Some snakes and lizards are not sensitive to α-Btx

† This work was supported by National Institutes of Health Grant NS 21896.
* Address correspondence to this author at the Department of Cell Biology, Yale University School of Medicine, 333 Cedar St., New Haven, CT 06510.

[1] Abbreviations: ACh, acetylcholine; AChR, acetylcholine receptor; α-Btx, α-bungarotoxin; κ-Btx, κ-bungarotoxin.

0006-2960/92/0431-1370$03.00/0